SOLSTICE:
An Electronic Journal of Geography and Mathematics

Persistent URL:
http://deepblue.lib.umich.edu/handle/2027.42/58219

Cite articles as:
Author names(s), Year. Title of article, *Solstice: An Electronic Journal of Geography and Mathematics*, Vol. XX, No. YY. Ann Arbor: Institute of Mathematical Geography.

Deep Blue | IMaGe Home | Solstice Home

Works best with a high speed internet connection.
Final version of IMaGe logo created by Allen K. Philbrick from original artwork from the Founder.

**VOLUME XXIV, NUMBER 2;
December, 2013**

Articles and Notes

Click on the cloud button to see a word cloud as an "abstract" of the adjacent article! Save any linked .kmz files on your computer and then open them in Google Earth.

Links of Interest

- From Joseph Kerski: Why Geography Education Matters
- From Rafael Pereira: If Christaller Had Google Earth...

In Memoriam: Alma S. Lach, 1914-2013. *Solstice* author. *Chicago Reader Blog* Obit with links elsewhere, including the *Chicago Sun-Times*.

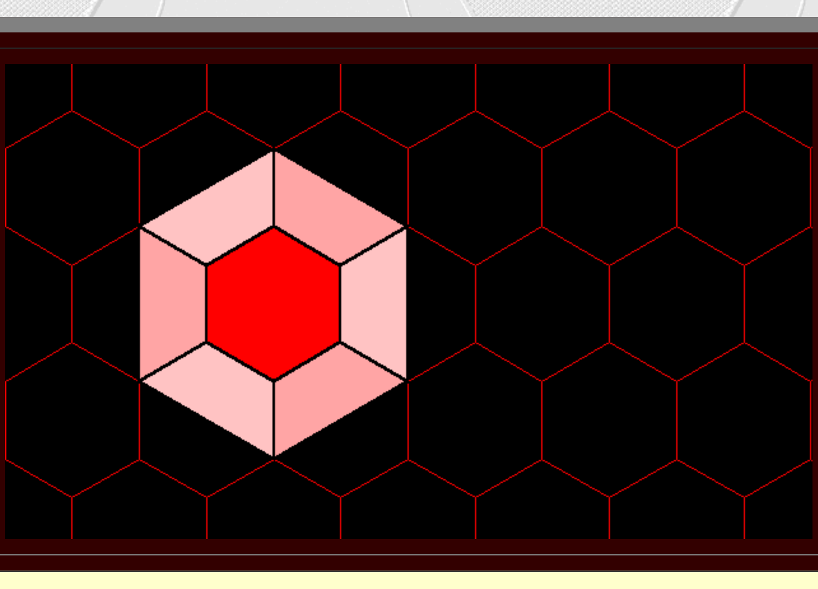

1. ARCHIVE
2. Editorial Board, Advice to Authors, Mission Statement
3. Awards

1. 2. 3.

RECENT NEWS, 2013

1. Chene Street History Project.
2. ***Spatial Mathematics: Theory and Practice Through Mapping***. Sandra L. Arlinghaus and Joseph Kerski, (2013), CRC Press. Linked video. Published July 2013,
3. The work above is the first volume in a series of books to be published by CRC Press in its series "**Cartography, GIS, and Spatial Science: Theory and Practice**." If you have an idea for a book to include, or wish to participate in some other way, please contact the series Editor, Sandra L. Arlinghaus.
4. Virtual Cemetery with William E. Arlinghaus; an ongoing project that continues in development run in the virtual world in parallel with the trust-funded model of a real-world cemetery.

Solstice was a Pirelli INTERNETional Award Semi-Finalist, 2001 (top 80 out of over 1000 entries worldwide)

One article in Solstice was a Pirelli INTERNETional Award Semi-Finalist, 2003 (Spatial Synthesis Sampler).

Solstice is listed in the Directory of Open Access Journals maintained by the University of Lund where it is maintained as a "searchable" journal.

Solstice is listed on the journals section of the website of the American Mathematical Society, http://www.ams.org/

Solstice is listed in *Geoscience e-Journals*

IMaGe is listed on the website of the Numerical Cartography Lab of The Ohio State University: http://ncl.sbs.ohio-state.edu/4_homes.html

---

Congratulations to all *Solstice* contributors.

Remembering those who are gone now but who contributed in various ways to *Solstice* or to IMaGe projects, directly or indirectly, during the first 28 years of IMaGe:

Allen K. Philbrick Alma S. Lach Donald F. Lach | Frank Harary | William D. Drake | H. S. M. Coxeter | Saunders Mac Lane | Chauncy D. Harris | Norton S. Ginsburg | Sylvia L. Thrupp | Arthur L. Loeb | George Kish |

1964 Boulder Drive,
Ann Arbor, MI 48104
734.975.0246
http://deepblue.lib.umich.edu/handle/2027.42/58219
sarhaus@umich.edu

A new topographic functional

Edward Earl and David Metzler

1 Introduction

The simplest and most familiar number associated to a mountain peak is the elevation of its summit above sea level. However, absolute elevation often does not correlate well with the visual impressiveness of a peak, which has more to do with the amount of local relief and the steepness of the flanks of the peak. For example, the summit of Mount Elbert, the highest point in the Rocky Mountains, is 4401 meters above sea level[1], while Devils Thumb[1], a striking rock spire on the border between Alaska and British Columbia, rises only to 2767 meters[2]. Based on pure elevation, Elbert far surpasses Devils Thumb. However, Mount Elbert rises from a high base in central Colorado, so its local relief is not nearly as great as its elevation would indicate; nor is it a particularly steep peak. For example, Elbert rises about 1600 meters (one mile) over a horizontal distance of 6.5 kilometers on its southeast flank[2]—which is not unimpressive. However, the northwest face of Devils Thumb soars an amazing 2000 meters in 1.6 km, and it is similarly steep in other directions. To get 2000 meters of vertical relief from the summit of Mount Elbert, one has to go about 30 km away, to the town of Aspen; if one goes 30 km from Devils Thumb, one gets to tidewater, yielding 2767 meters of relief. See Table 1 for representative profiles of the two peaks; also see topographical maps for Mount Elbert and for Devils Thumb.[3]

In this article we introduce a functional that takes into account the relief and steepness of a peak in a mathematically elegant way, and which has substantial correlation with the visual impressiveness of the peak. In fact, our functional can be applied to any point on a landscape (not necessarily a summit—for example, see the discussion below of the famous granite cliff of El Capitan in Yosemite), or indeed, any point on the graph of a function. We will also briefly introduce two concepts derived from the main functional; one takes into account how independent a particular feature is from nearby "better" features, and the other calculates a kind of "ruggedness" for a domain.

A pedagogical note: using the basic definitions provides good exercises in multivariable calculus, suitable for strong students in an introductory course. Proving theorems about these measures involve good workouts with elementary real and functional analysis.

[1] There is no apostrophe in the official spelling of the name of this peak.

[2] One can verify these numbers using the public-domain mapping website mapper.acme.com, among others.

[3] Google Earth produces a good virtual tour of Mount Elbert. However it has very inaccurate (and misleadingly smoothed-out) elevation data for Devils Thumb. Getting accurate elevation data for steep features in obscure locations, such as Devils Thumb, is one of the challenges of this research.

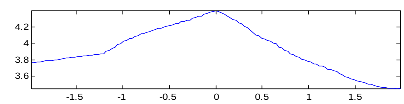

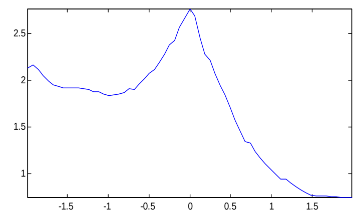

Table 1: Mount Elbert (left) and Devils Thumb (right) profiles

2 Omnidirectional Relief and Steepness (ORS)

Let $h : \mathbb{R}^2 \to \mathbb{R}$ be a bounded, Lebesgue measurable function, thought of as the height function of a landscape. (We do not require h to be continuous, to permit the presence of vertical cliffs.[4]) Consider a fixed *base point* $\mathbf{p} \in \mathbb{R}^2$, and a corresponding *reference point* $(\mathbf{p}, h_0)$. (It is theoretically useful, and no more complicated, to let the height h_0 of the reference point vary independently, so h_0 need not equal $h(\mathbf{p})$. Physically, one can imagine, for example, $h_0 > h(\mathbf{p})$ to be the height of the top of a flagpole placed atop a peak. However we will primarily be interested in the case where $h_0 = h(\mathbf{p})$.) We will define a functional of this data, which we call *omnidirectional relief and steepness* (ORS), which will capture a kind of average of the relief and steepness of the terrain as viewed from the reference point.

More precisely, let $h \in L^\infty\left(\mathbb{R}^2\right)$, and let $(\mathbf{p}, h_0) \in \mathbb{R}^2 \times \mathbb{R}$. We will presently define ORS of the reference point $(\mathbf{p}, h_0)$ relative to the landscape h, yielding a functional

$$\begin{gathered} \mathrm{ORS} : \mathbb{R}^2 \times \mathbb{R} \times L^\infty\left(\mathbb{R}^2\right) \to \mathbb{R} \\ (\mathbf{p}, h_0; h) \mapsto \mathrm{ORS}\left(\mathbf{p}, h_0; h\right) \end{gathered}$$

(In fact we will define a whole family of possible functionals, but we will immediately specialize to one particularly appealing case.)

We first consider a simple landscape, both to fix ideas and to define an important normalization for the general case. It is a radially symmetrical conical peak, rising from a flat plain. Given a point $\mathbf{x} \in \mathbb{R}^2$, denote the distance from

[4] We could use S^2 as the domain, to take into account the spherical nature of the Earth, but we will see that all of the calculations localize strongly, making the difference minuscule. Generalizing everything in this paper to $\mathbb{R}^n$ is straightforward, but we use $\mathbb{R}^2$ throughout for simplicity and because of the application to physical landscapes. However, we do not take into account overhanging cliffs, since that would vastly complicate the mathematical model.

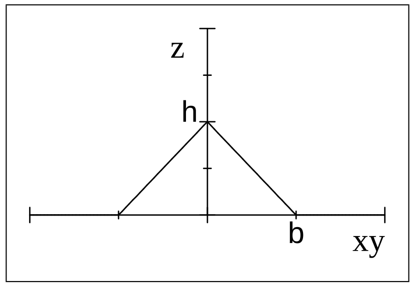

Figure 1: Cross-section of cone function with height 1 and slope 1

the origin to $\mathbf{x}$ by $r(\mathbf{x})$, or just r for short (i.e. it is the usual r of polar coordinates).

Definition 1 *Let $h_0, b > 0$, let $s = h_0/b$, and let $\phi = \arctan s$. Then the **cone function** $c : \mathbb{R}^2 \to \mathbb{R}$ associated to h_0, b is given by*

$$c(\mathbf{x}) = \begin{cases} h_0 - sr, & r < b \\ 0 & r > b \end{cases}$$

(We suppress the dependence on h_0, b for tidiness.) Note that s is the slope of the cone, and ϕ is the angle its sides make with the xy-plane.

See Figure 1 for the cross-section of the cone. We wish to define the ORS of the summit of this cone, i.e. $\mathrm{ORS}(\mathbf{0}, h_0; c)$. It should take into account its height, and also its steepness. The combination $h_0 s$ does not work, since it is unbounded for large s, even if h_0 is small. The combination $h_0\phi$ is just as natural, and is bounded. We will actually choose $\frac{2}{\pi}h_0\phi$ ("height times angle over 90°"), so that the limiting case $\phi \to \pi/2$, which we will call a *flagpole*, yields simply h_0. Hence we have the following.

Definition 2 *We say that ORS is **angle-normalized** if it yields $\frac{2}{\pi}h_0\phi$ when applied to the vertex of the cone with height h and angle ϕ:*[5]

$$\mathrm{ORS}(\mathbf{0}, h_0; c) = \frac{2}{\pi}h_0\phi$$

Note two further important features of the conical case: first, if two cone functions c_1, c_2 share the same angle but have different heights $h_2 = Ah_1$, then the ORS of c_2 will be A times the ORS of c_1. In other words, scaling up every dimension (heights and horizontal distances) by a factor of A results in scaling

[5] We discuss other possible normalizations just after Theorem 5.

up ORS by the same factor. We will see below that this homogeneity, or scale-covariance, property is true of ORS in general; in particular, it means that ORS has meaningful units, namely, units of length. (In the topographic examples below, ORS is given in meters.)

Second, if we take a low-slope cone c with height h and base $b >> h$ and scale up h by a factor of A, leaving b unchanged, then the ORS will increase by approximately A^2. This low-slope quadratic behavior is also a general feature of ORS.

Now we turn to the general case of a non-conical peak or other topographic feature. We imagine standing at the reference point—say the summit of a mountain—and looking down in all directions, gauging the impressiveness of the view. We want to take some sort of average of the impressiveness information obtained by looking in all directions. One can also think of stationing a host of tourists (mathematically, these will be called *sample points*) everywhere around the mountain, all looking up at the summit, and surveying them for their idea of the impressiveness of the summit.[6] Hence ORS will involve an integral over the set of all sample points; we will denote a typical sample point by $\mathbf{x}$, and we will set $r = \|\mathbf{p} - \mathbf{x}\|$, the distance from the reference point to a sample point.

For every sample point $\mathbf{x}$, we calculate the slope $u(\mathbf{x}) = (h_0 - h(\mathbf{x}))/r$. If we integrated u itself, the integral over all $\mathbf{x} \in \mathbb{R}^2$ would clearly diverge for most landscapes. Instead, we use an appropriate function to turn u into a sensible integrand. We first present a general definition, using an arbitrary such function, and then use the cone normalization to determine what function we desire.

Definition 3 *Let $f : \mathbb{R} \to \mathbb{R}$ be a continuous function with $f(u) = 0$ for $u \leq 0$.*[7] *Let $h \in L^\infty(\mathbb{R}^2)$, and let $(\mathbf{p}, h_0) \in \mathbb{R}^2 \times \mathbb{R}$. Let $r = \|\mathbf{x} - \mathbf{p}\|$ be the radial coordinate based at $\mathbf{p}$, and let $u(\mathbf{x}) = (h_0 - h(\mathbf{x}))/r$. The* ***omnidirectional relief and steepness (ORS)*** *of the reference point $(\mathbf{p}, h_0)$ relative to the landscape h, using f, is*

$$\begin{aligned}
\mathrm{ORS}_f(\mathbf{p}, h_0; h) &= \|f \circ u\|_2 \\
&= \left[\iint_{\mathbb{R}^2} f^2 \left(\frac{h_0 - h(\mathbf{x})}{r} \right) dA(\mathbf{x}) \right]^{1/2}
\end{aligned}$$

Before examining the general properties of ORS, we first derive the correct function f based on our normalization.

[6] Note that ORS ignores line-of-sight issues: we make no distinction between points that are actually in view from the reference point and points that are obscured by intervening terrain. Hence phrases such as "looking up at the mountain" should not be taken too literally.

[7] It is not absolutely necessary to require that f vanish for negative u. It has the effect of ignoring surrounding higher terrain in evaluating the reference point. This usually has a negligible effect when the reference point is a summit, which is our main application. Dropping this requirement turns out to make the reduced version of ORS, discussed at the end of this paper, difficult to define.

Proposition 4 *Let $f:\mathbb{R}\to\mathbb{R}$ be differentiable and assume that $f(u)=o(u^{1+\varepsilon})$ for some $\varepsilon>0$, as $u\to 0$. Let $h_0, b>0$ and let c be the associated cone function, with slope $s=h_0/b$. Then $\mathrm{ORS}_f(\mathbf{0},h_0;c)=h_0F(s)$, where F satisfies the initial value problem*

$$\frac{1}{\pi}\left(F^2(s)\right)'=\frac{1}{s^2}\left(f^2(s)\right)',\qquad F(0)=0.$$

Proof. Defining F as in the theorem, we have

$$\begin{aligned}
h_0F(s) &= \left(\iint\limits_{\mathbb{R}^2} f^2\left(\frac{h_0-c(r)}{r}\right)dA\right)^{1/2}\\
h_0^2F^2(s) &= 2\pi\int_0^\infty f^2\left(\frac{h_0-c(r)}{r}\right)r\ dr.\\
\frac{1}{2\pi}h_0^2F^2(s) &= \int_0^b f^2\left(s\right)r\ dr+\int_b^\infty f^2\left(\frac{h_0}{r}\right)r\ dr\\
&= \frac{1}{2}f^2\left(s\right)b^2+\int_0^s f^2\left(u\right)\frac{h_0^2}{u^3}\ du
\end{aligned}$$

where we have set $u=h_0/r$ and hence $du=-\left(h_0/r^2\right)dr$ or $r\ dr=-\left(r^3/h_0\right)\ du=-\left(h_0^2/u^3\right)\ du$. Note that the order of vanishing assumed for f makes all the integrals converge. Hence

$$\begin{aligned}
\frac{1}{2\pi}h_0^2F^2(s) &= \frac{1}{2}f^2(s)\frac{h_0^2}{s^2}+\int_0^s f^2(u)\frac{h_0^2}{u^3}\ du\\
\frac{1}{2\pi}F^2(s) &= \frac{1}{2s^2}f^2(s)+\int_0^s f^2(u)\frac{du}{u^3}
\end{aligned}$$

Integration by parts yields

$$\begin{aligned}
\frac{1}{2\pi}F^2(s) &= \frac{1}{2s^2}f^2(s)-\frac{1}{2s^2}f^2(s)\\
&\quad+\lim_{u\to 0}\frac{f^2(u)}{2u^2}+\frac{1}{2}\int_0^s\left(f^2(u)\right)'\frac{du}{u^2}\\
&= \frac{1}{2}\int_0^s\left(f^2(u)\right)'\frac{du}{u^2}
\end{aligned}$$

or, taking the derivative of both sides,

$$\frac{1}{\pi}\left(F^2(s)\right)'=\frac{1}{s^2}\left(f^2(s)\right)',\qquad F(0)=f(0)=0.$$

■

Proposition 5 *Let*

$$f(u)=\left[\frac{4}{\pi^3}\left(2u\arctan u-\ln\left(u^2+1\right)-\arctan^2 u\right)\right]^{1/2}\tag{1}$$

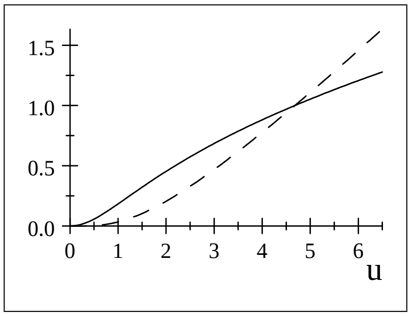

Figure 2: Plot of f (solid) and f^2 (dashed)

for $u \geq 0$ and $f(u) = 0$ for $u < 0$. Then the function F associated to f by Proposition 4 is $F(s) = \frac{2}{\pi}\arctan s$, and hence the resulting ORS_f is angle-normalized:

$$\mathrm{ORS}_f(\mathbf{0}, h_0; c) = \frac{2}{\pi} h_0 \phi.$$

Proof.

$$\begin{aligned}
f^2(s) &= \frac{1}{\pi}\int_0^s u^2 \left(F^2(u)\right)' \, du \\
&= \frac{4}{\pi^3}\int_0^s u^2 \left(\arctan^2 u\right)' \, du \\
&= \frac{8}{\pi^3}\int_0^s \frac{u^2}{u^2+1} \arctan u \, du \\
&= \frac{8}{\pi^3}\int_0^s \left(1 - \frac{1}{u^2+1}\right) \arctan u \, du \\
&= \frac{4}{\pi^3}\left[2\int_0^s \arctan u \, du - \int_0^s \left(\arctan^2 u\right)' \, du\right] \\
&= \frac{4}{\pi^3}\left[2u \arctan u|_0^s - 2\int_0^s \frac{u}{u^2+1} \, du - \arctan^2 s\right] \\
&= \frac{4}{\pi^3}\left[2s \arctan s - \ln\left(s^2+1\right) - \arctan^2 s\right].
\end{aligned}$$

■

We exclusively use this angle-normalized f, shown in Figure 2, in our calculations of ORS in this paper. However we can say a word about what happens when one chooses different functions for f. Since ORS combines information about local relief with information about steepness, there is an issue of how much to weight relief versus steepness: should we assign a greater value to a very steep, but only moderately high peak, or to a moderately steep, but very high peak? At the risk of making apples-to-oranges comparisons, we boldly proceed to assign one number that makes a certain tradeoff between relief and steepness. Different choices for f will result in somewhat different tradeoffs, either more "heightist" (favoring relief over steepness) or more "slopist" (the opposite). In past work we have also tried other normalizations, notably $F(s) = s/(s+1)$, which is more heightist than the angle normalization. We work with angle normalization for reasons of simplicity, elegance, and a good fit with visual impressiveness.

For the remainder of this paper, we will use the modified slope integrand f given in Theorem 5, and we will suppress f from the notation; that is, we define

$$\mathrm{ORS}(\mathbf{p}, h_0; h) = \mathrm{ORS}_f(\mathbf{p}, h_0; h)$$

With this definition, ORS has many good properties, including strong versions of continuity, which are essential for dealing with the discretized data encountered in practice.[8] Note that the square root in the definition is an order-preserving function; hence for the purposes of comparing peaks (one of our main uses for ORS), it is enough to use ORS^2, which will be simpler to analyze. One can think of the square root serving mainly to make normalization easier (in particular, it produces a quantity with units of length). The root does make it tricky to analyze the behavior of ORS for landscapes where ORS is very small. This is not a major concern for our purposes, since we focus primarily on reference points for which ORS is relatively large. Also, taking the square root halves relative error, so any relative error result for ORS^2 yields a corresponding, and stronger, relative error result for ORS.

Proposition 6 *The functional* $\mathrm{ORS} : \mathbb{R}^2 \times \mathbb{R} \times L^\infty\left(\mathbb{R}^2\right) \to \mathbb{R}$ *has the following properties:*

1. ORS *is weakly increasing as a function of* h_0 *and weakly decreasing as a function of* h*: for every* $\mathbf{p} \in \mathbb{R}^2$*,* $h_0, k_0 \in \mathbb{R}$*, and* $h, k \in L^\infty$*, if* $h_0 \leq k_0$ *and* $h \geq k$*, then* $\mathrm{ORS}(\mathbf{p}, h_0; h) \leq \mathrm{ORS}(\mathbf{p}, k_0; k)$*.*

2. ORS *is bounded by the maximum height of the landscape: for every* $\mathbf{p} \in \mathbb{R}^2$*,* $h_0 \in \mathbb{R}$*, and* $h \in L^\infty$*,* $\mathrm{ORS}(\mathbf{p}, h_0; h) \leq \|h_0 - h\|_\infty$*. In particular, it is finite for any bounded landscape and any reference point.*

3. ORS *is invariant under vertical translation and horizontal translation: for every* $\mathbf{p} \in \mathbb{R}^2$*,* $h_0 \in \mathbb{R}$*,* $h \in L^\infty$*,* $a \in \mathbb{R}$*, and* $\mathbf{q} \in \mathbb{R}^2$*,*

$$\begin{aligned} \mathrm{ORS}(\mathbf{p}, h_0 + a; h + a) &= \mathrm{ORS}(\mathbf{p}, h_0; h) \\ \mathrm{ORS}(\mathbf{p} + \mathbf{q}, h_0; h(\mathbf{x} - \mathbf{q}) &= \mathrm{ORS}(\mathbf{p}, h_0; h) \end{aligned}$$

4. ORS *is invariant under reflections and rotations about the reference point: let* A *be a 2 by 2 orthogonal matrix and define* $h_A(\mathbf{x}) = h(A(\mathbf{x} - \mathbf{p}) + \mathbf{p})$*. Then*

$$\mathrm{ORS}(\mathbf{p}, h_0; h_A) = \mathrm{ORS}(\mathbf{p}, h_0; h)$$

[8] In particular, the Lipschitz continuity in Corollary 13 would not hold if we used a 1-norm instead of a 2-norm, which might otherwise seem simpler.

5. ORS_f *is scale-covariant (if we scale the landscape both horizontally and vertically), and in particular it has units of length. That is, if* h_M *is obtained from* h *by dilating horizontally about the point* $\mathbf{p}$ *by* $M > 0$ *and scaling vertically by* M *(i.e.* $h_M(\mathbf{x}) = M \cdot h\left((\mathbf{x} - \mathbf{p})/M + \mathbf{p}\right)$*) then*

$$\mathrm{ORS}(\mathbf{p}, Mh_0; h_M) = M \cdot \mathrm{ORS}(\mathbf{p}, h_0; h)$$

Proof. Monotonicity (1) and vertical and horizontal translation invariance (3) are clear from the definition. Invariance under reflections and rotations follows from the corresponding invariance of the integral. Scale-covariance follows from the change of variables indicated in item 5. The bound given in item 2 follows from monotonicity and the flagpole case of the cone normalization; hence we will refer to this bound as the flagpole bound. ■

Remark 7 *By using vertical and horizontal invariance, we can always reduce to the case where the reference point is the origin and the reference height is zero. We do this below for simplicity, denoting the result by* $\mathrm{ORS}(h) = \mathrm{ORS}(\mathbf{0}, 0; h)$*. Note that in any statement involving a variation of the landscape* h*, we can recover a more general version, with variation in* h_0 *as well: for example, simply replace any quantity of the form* $\|h - k\|_\infty$ *by* $\|(h_0 - h) - (k_0 - k)\|$.

Before turning to results about the continuity and robustness of ORS, we need a lemma about the function f which appears in the definition. This lemma summarizes all of the features of f that are necessary for the results about ORS that follow.

Lemma 8 *The function* f *defined in Proposition 5 is* C^1 *on* $\mathbb{R}$ *and has the following properties for* $u > 0$*. (Recall that* f *is identically zero for* $u \leq 0$*.)*

1. f *is strictly increasing.*
2. $f^2(u) = \frac{2}{\pi^3}u^4 + O(u^6)$.
3. $f(u) = \sqrt{\frac{2}{\pi^3}} \cdot u^2 + O(u^3)$ *as* $u \to 0^+$ *and* $f(u) \leq \min\left\{\sqrt{\frac{2}{\pi^3}} \cdot u^2, \frac{2}{\pi}\sqrt{u}\right\}$.
4. f^2 *is strictly convex.*
5. $0 \leq \left(f^2\right)'(u) < \frac{4}{\pi^2}$ *and* $\left(f^2\right)'(u) \leq \frac{8}{\pi^3}u^3$.

Proof. Let $u > 0$. The function

$$f^2(u) = \frac{4}{\pi^3}\left(2u \arctan u - \ln\left(u^2 + 1\right) - \arctan^2 u\right)$$

is clearly C^∞. Its Taylor expansion at $u = 0$ is

$$\begin{aligned} f^2(u) &= \frac{4}{\pi^3}\left(2u\left(u - \frac{u^3}{3}\right) - \left(u^2 - \frac{u^4}{2}\right) - \left(u - \frac{u^3}{3}\right)^2\right) + O(u^6) \\ &= \frac{2}{\pi^3}u^4 + O(u^6) \end{aligned}$$

Hence

$$\begin{aligned} f(u) &= \sqrt{\frac{2}{\pi^3}u^4\left(1+O\left(u^2\right)\right)} \\ &= \sqrt{\frac{2}{\pi^3}}u^2\left(1+O(u^2)\right) \end{aligned}$$

This shows that, even with the proviso that $f(u)=0$ for $u<0$, f is C^1 for all $u\in\mathbb{R}$.

Next we calculate the derivative of the squared function:

$$\left(f^2\right)'(u) = \frac{8}{\pi^3}u^2\frac{\arctan u}{u^2+1}$$

(recall from Prop.4 that it is not accidental that this is relatively simple). This is clearly positive for $u>0$; hence f^2 and f are both increasing (in fact, strictly increasing as long as $u>0$). (Again, this follows also from Prop. 4.) Since $\arctan u < \min\left\{\frac{\pi}{2}, u\right\}$ for $u>0$, we see also that $\left(f^2\right)'(u) < \min\left\{\frac{4}{\pi^2}, \frac{8}{\pi^3}u^3\right\}$ for $u>0$. We take the second derivative and obtain

$$0 < \left(f^2\right)''(u) = \frac{8}{\pi^3}\frac{u\left(u+2\arctan u\right)}{\left(u^2+1\right)^2} < \frac{24}{\pi^3}u^2 = \frac{d^2}{du^2}\left(\frac{2}{\pi^3}u^4\right) \qquad (u>0)$$

which shows that $\left(f^2\right)$ is convex, and also, since $f^2(0)=\left(f^2\right)'(0)=0$, that

$$f^2(u) < \frac{2}{\pi^3}u^4$$

and hence that

$$f(u) < \sqrt{\frac{2}{\pi^3}}u^2$$

as desired. ■

We now consider the sensitivity of ORS and ORS^2 to the landscape data h (and hence also to the height h_0 of the reference point, as in Remark 7). We certainly want continuity, but we actually want a bit more; continuous functions can have unpleasantly large derivatives. This is important when dealing with discrete, and often somewhat inaccurate, digital data. In fact, a previous attempt at defining such a function using a 1-norm instead of a 2-norm led to poor behavior in this regard.

To quantify the sensitivity of ORS$^2(h)$ to variations in h, we recall the following standard notion from functional analysis.[3]

Definition 9 *Given a function $F:V\to W$ between two topological vector spaces, the Gâteaux differential of F is the function dF given by*

$$dF(h,v) = \left.\frac{d}{dt}\right|_{t=0} F(h+tv)$$

F is said to be Gâteaux differentiable at $h\in V$ if dF exists for all $v\in V$.

In general, dF need not be continuous or linear. In our case, we are most interested in the following. Suppose that V and W are Banach spaces, and that F is Gâteaux differentiable at h. Then define

$$mF(h) = \sup_{\|v\|=1} \|dF(h,v)\|$$

(which may be infinite). If F is actually (Fréchet) differentiable at h, this is clearly just the norm of the derivative, as a linear operator between Banach spaces. It measures the worst-case sensitivity of F at h. We are interested in a simpler quantity, namely

$$MF(H) = \sup_{\|h\|=H} mF(h) = \sup_{\|h\|=H} \sup_{\|v\|=1} \|dF(h,v)\|$$

which gives the worst-case sensitivity of F over all inputs of given norm H. We are interested in the case where $V = L^\infty$ and $W = \mathbb{R}$. For example, if $F(h) = \|h\|_\infty^2$, a simple calculation yields $MF(H) = 2H$. With this notation, we can state our main result about the sensitivity of ORS.

Theorem 10 *The worst-case sensitivity of* ORS^2 *satisfies*

$$M\mathrm{ORS}^2(H) = 2H$$

That is, it is exactly as sensitive, in the worst case, as the function H^2. For ORS *itself, we have*

$$m\mathrm{ORS}(h) \leq \frac{\|h\|_\infty}{\mathrm{ORS}(h)}$$

Before proving the theorem, we first note the following easy consequence of monotonicity, whose proof we omit.

Lemma 11 *Let $H > 0$ be fixed and consider all pairs of landscapes $h, k \in L^\infty$, with $\|h-k\|_\infty = H$. Then $\left|\mathrm{ORS}^2(h) - \mathrm{ORS}^2(k)\right|$ is maximized when $h-k$ is a constant function (a.e.).*

Proof of the Theorem. Let $h \in L^\infty$. By the lemma, to calculate $m\mathrm{ORS}(h)$, we need only consider the case where v is constant function; let's say $v = z$ everywhere. So

$$\begin{aligned}
m\mathrm{ORS}(h) &= \left.\frac{d}{dz}\right|_{z=0} \mathrm{ORS}_f^2(h+z) \\
&= \left.\frac{d}{dz}\right|_{z=0} \int_{\mathbb{R}^2} f^2\left(\frac{h(\mathbf{x})+z}{r}\right) dA \\
&= \int_{\mathbb{R}^2} \left.\frac{\partial}{\partial z}\right|_{z=0} \left(f^2\left(\frac{h(\mathbf{x})+z}{r}\right)\right) dA \\
&= \int_{\mathbb{R}^2} (f^2)'\left(\frac{h(\mathbf{x})}{r}\right) \frac{1}{r}\, dA
\end{aligned}$$

where we can pass the derivative inside the integral since $\left(f^2\right)'\left(\frac{h(\mathbf{x})}{r}\right)\frac{1}{r}$ is integrable.[4] (It is integrable near the origin since $\left(f^2\right)'$ is bounded, and at infinity since $\left(f^2\right)'(u) \leq \frac{8}{\pi^3}u^3$, both by Lemma 8.) Now let $H > 0$ and consider all functions h with $\|h\|_\infty = H$. Since $\left(f^2\right)'$ is increasing by Lemma 8, $m\mathrm{ORS}(h)$ will be maximized when h is a constant function, with value H. But this reduces us to the case where $h = H$ and v are both constant, that is, the flagpole case, and this is normalized to give

$$\mathrm{ORS}^2(H) = H^2$$

for which we have already noted that

$$M\mathrm{ORS}^2(H) = 2H$$

The result about ORS itself follows by the chain rule:

$$\begin{aligned}
m\mathrm{ORS}(h) &= \left.\frac{d}{dz}\right|_{z=0}\sqrt{\mathrm{ORS}^2(h+z)} \\
&= \frac{\left.\frac{d}{dz}\right|_{z=0}\mathrm{ORS}^2(h+z)}{2\sqrt{\mathrm{ORS}^2(h)}} \\
&\leq \frac{M\mathrm{ORS}^2(\|h\|_\infty)}{2\sqrt{\mathrm{ORS}^2(h)}} \\
&= \frac{\|h\|_\infty}{\sqrt{\mathrm{ORS}^2(h)}}
\end{aligned}$$

■

Corollary 12 *The function* ORS^2 *is locally Lipschitz continuous, and the Lipschitz bound depends only on* $\|h\|_\infty$*. More precisely, on any set* S *with* $\|h\|_\infty \leq H$ *for all* $h \in S$*,*

$$\left|\mathrm{ORS}^2\left(h_0\right) - \mathrm{ORS}^2\left(h_1\right)\right| \leq 2H$$

for all h_0, h_1 *in* S*.*

Proof. For $h_0, h_1 \in S$, let $h_t = th_1 + (1-t)\,h_0$. The corollary follows from the mean value theorem applied to the function $t \mapsto \mathrm{ORS}^2\left(h_t\right)$, since the preceding theorem implies that the derivative of this function is bounded by $2H$. ■

Corollary 13 *The function* ORS *is continuous, and it is locally Lipschitz continuous away from the zero (a.e.) landscape. Further, on a set* S *on which* ORS *is bounded away from zero,* ORS *is uniformly Lipschitz continuous.*

Proof. ORS is continuous since ORS^2 is. If h is not the zero landscape, then $\mathrm{ORS}\,(h) \neq 0$, and by continuity, there is a neighborhood around h where ORS is bounded away from zero. Hence a mean value theorem argument as in the last corollary, using the bound on $m\mathrm{ORS}\,(h)$ in the theorem, yields local Lipschitz continuity. If ORS is bounded away from zero a priori, then the same argument gives a uniform Lipschitz constant. ■

Remark 14 *Even for landscapes with small* ORS *values, ORS tends to be better-behaved than this corollary would indicate, but the result given is satisfactory for our purposes.*

While the previous theorem and its corollaries address the sensitivity of ORS to an arbitrary bounded change in the landscape, we get a sharper result if the change in the landscape occurs only far away from the reference point. This is important to the interpretation of ORS as a measure of local impressiveness, without regard to absolute elevation above the level of a distant ocean. As before, it is simpler to discuss ORS^2.

Theorem 15 (Locality) ORS^2 *is local: the contribution I to $\mathrm{ORS}^2(h)$ from points $\mathbf{x}$ with $\|\mathbf{x}\| > R$ satisfies*

$$I \le \frac{2\,\|h\|_\infty^4}{\pi^2 R^2}.$$

Hence for every $h, k \in L^\infty$, if $h(\mathbf{x}) = k(\mathbf{x})$ for all $\mathbf{x}$ with $\|\mathbf{x}\| \le R$, and $\|h\|_\infty, \|k\|_\infty \le H$, then

$$\left|\mathrm{ORS}^2(h) - \mathrm{ORS}^2(k)\right| \le \frac{2H^4}{\pi^2 R^2}$$

Proof. Let $E = \left\{\mathbf{x} \in \mathbb{R}^2 : \|\mathbf{x}\| \ge R\right\}$. Then

$$\begin{aligned}
I &= \int_E f^2(h(\mathbf{x})/r)\; dA \\
&\le \frac{2}{\pi^3}\int_E \left(\frac{h(\mathbf{x})}{r}\right)^4 \; dA \\
&= \frac{2}{\pi^3}\int_0^{2\pi}\int_R^\infty \left(\frac{h(\mathbf{x})}{r}\right)^4 \; r dr d\theta \\
&\le \frac{4}{\pi^2}\int_R^\infty \frac{\|h\|_\infty^4}{r^3}\; dr \\
&\le \frac{2\,\|h\|_\infty^4}{\pi^2 R^2}
\end{aligned}$$

■

We noted above that in the case of a low-slope cone, ORS is approximately quadratic in the height (for a fixed base radius) This is true in general as long as the slopes near the reference point are bounded.

Theorem 16 *For terrain that has bounded slope near the origin,* ORS(h) *approximately scales quadratically in the height (with no horizontal scaling). More precisely, assume that $h(\mathbf{x})/r$ is bounded and let $M > 0$. Then*

$$\mathrm{ORS}(Mh) = CM^2 + O(M^4)$$

as $M \to 0$, for some C depending on h.

Proof. Let $u(\mathbf{x}) = -h(\mathbf{x})/r$ and let $H = \|h\|_\infty$. Then the corresponding slope function for the (vertically) scaled landscape is Mu, and

$$\begin{aligned}
\mathrm{ORS}^2(Mh) &= \int_{\mathbb{R}^2} f^2(Mu(\mathbf{x}))\ dA \\
&= \int_{\mathbb{R}^2} \left[\frac{2}{\pi^3} M^4 u(\mathbf{x})^4 + g\left(Mu(\mathbf{x})\right)\right]\ dA \\
&= \frac{2}{\pi^3} M^4 \int_{\mathbb{R}^2} u(\mathbf{x})^4\ dA + \int_{\mathbb{R}^2} g\left(Mu(\mathbf{x})\right)\ dA
\end{aligned}$$

where $|g(u)| \le C_1 u^6$ for all u. Hence

$$\begin{aligned}
\left|\mathrm{ORS}^2(Mh) - \frac{2}{\pi^3} M^4 \int_{\mathbb{R}^2} u(\mathbf{x})^4\ dA\right| &\le \left|\int_{\mathbb{R}^2} g\left(Mu(\mathbf{x})\right)\ dA\right| \\
&\le \int_{\mathbb{R}^2} \left|g\left(Mu(\mathbf{x})\right)\right|\ dA \\
&\le \int_{\mathbb{R}^2} C_1 M^6 u(\mathbf{x})^6\ dA
\end{aligned}$$

Since h is bounded, u decays at least as $1/r$ at infinity, and it is assumed to be bounded at the origin. Hence

$$\int_{\mathbb{R}^2} u(\mathbf{x})^n\ dA < \infty \quad \text{for } n \ge 3$$

We can apply this for $n = 4$ to the expression above to see that

$$C_2 = \frac{2}{\pi^3} \int_{\mathbb{R}^2} u(\mathbf{x})^4\ dA$$

is finite. Applying the case $n = 6$ gives

$$\left|\mathrm{ORS}^2(Mh) - C_2 M^4\right| \le C_3 M^6$$

where $C_3 = C_1 \int_{\mathbb{R}^2} u(\mathbf{x})^6\ dA$. Therefore

$$\mathrm{ORS}^2(Mh) = C_2 M^4 + O(M^6)$$

and

$$\mathrm{ORS}(Mh) = CM^2 + O(M^4)$$

as desired, where $C = \sqrt{C_2}$. ■

To state the next result, we return to considering ORS as a function of $\mathbf{p}$, h_0, and h. We look at how ORS depends on the horizontal location of the reference point, if we do not change its height. (This is a little strange physically, as the reference point is usually at ground level; we will address this immediately after the theorem.)

Theorem 17 *Let $H > 0$ be fixed. Then* ORS^2 *and ORS are continuous in* $\mathbf{p}$*, uniformly in* $\mathbf{p}$*,* h_0*, and* h*, provided that* $\|h_0 - h\|_\infty \leq H$*.*

We first need a lemma regarding $f^2(h/r)$.

Lemma 18 *Given r_1, r_2 with $0 < r_1 < r_2$, $f^2(h/r_1) - f^2(h/r_2)$ is an increasing function of h for $h \geq 0$.*

Proof. We have

$$\begin{aligned}
\frac{d}{dh}\left(f^2\left(\frac{h}{r_1}\right) - f^2\left(\frac{h}{r_2}\right)\right) &= \left(f^2\right)'\left(\frac{h}{r_1}\right)\frac{1}{r_1} - \left(f^2\right)'\left(\frac{h}{r_2}\right)\frac{1}{r_2} \\
&> \frac{1}{r_1}\left(\left(f^2\right)'\left(\frac{h}{r_1}\right) - \left(f^2\right)'\left(\frac{h}{r_2}\right)\right) \\
&> 0
\end{aligned}$$

since f^2 is convex. ■

Proof of the Theorem. We wish to bound $\left|\mathrm{ORS}^2(\mathbf{q}, h_0; h) - \mathrm{ORS}^2(\mathbf{p}, h_0; h)\right|$ for $\mathbf{q}$ near $\mathbf{p}$. Without loss of generality, we can let $\mathbf{p}$ be the origin, $h_0 = 0$, and $\mathbf{q} = (\delta, 0)$, for some $\delta > 0$, and we can look at the case where $\mathrm{ORS}^2(\mathbf{q}, h_0; h) \geq \mathrm{ORS}^2(\mathbf{p}, h_0; h)$. We have

$$\begin{aligned}
\mathrm{ORS}^2(\mathbf{q}, 0; h) - \mathrm{ORS}^2(\mathbf{0}, 0; h) &\leq \int_{\mathbb{R}^2}\left(f^2\left(\frac{h(\mathbf{x})}{\|\mathbf{x}-\mathbf{q}\|}\right) - f^2\left(\frac{h(\mathbf{x})}{r}\right)\right) dA \\
&= \int_{\frac{\delta}{2}}^{\infty}\int_{-\infty}^{\infty}\left(f^2\left(\frac{h(\mathbf{x})}{\|\mathbf{x}-\mathbf{q}\|}\right) - f^2\left(\frac{h(\mathbf{x})}{r}\right)\right) dy\, dx \\
&\quad + \int_{-\infty}^{\frac{\delta}{2}}\int_{-\infty}^{\infty}\left(f^2\left(\frac{h(\mathbf{x})}{\|\mathbf{x}-\mathbf{q}\|}\right) - f^2\left(\frac{h(\mathbf{x})}{r}\right)\right) dy\, dx \\
&\leq \int_{\frac{\delta}{2}}^{\infty}\int_{-\infty}^{\infty}\left(f^2\left(\frac{h(\mathbf{x})}{\|\mathbf{x}-\mathbf{q}\|}\right) - f^2\left(\frac{h(\mathbf{x})}{r}\right)\right) dy\, dx
\end{aligned}$$

where the second integral drops out because $\|\mathbf{x} - \mathbf{q}\| > r$ on that region and $f^2(h/r)$ is a decreasing function of r. Also, by the previous lemma, the difference between the f^2 values at a particular $\mathbf{x}$ will be maximized when $h(\mathbf{x})$ is as large as possible, so we have

$$
\begin{aligned}
\mathrm{ORS}^2(\delta,0,0;h)-\mathrm{ORS}^2(0,0,0;h) &\le \int_{\frac{\delta}{2}}^{\infty}\int_{-\infty}^{\infty}\left(f^2\left(\frac{H}{\|\mathbf{x}-\mathbf{q}\|}\right)-f^2\left(\frac{H}{r}\right)\right)\,dy\,dx\\
&= \int_{-\frac{\delta}{2}}^{\infty}\int_{-\infty}^{\infty} f^2\left(\frac{H}{r}\right)\,dy\,du-\int_{\frac{\delta}{2}}^{\infty}\int_{-\infty}^{\infty} f^2\left(\frac{H}{r}\right)\,dy\,dx\\
&= \int_{-\frac{\delta}{2}}^{\frac{\delta}{2}}\int_{-\infty}^{\infty} f^2\left(\frac{H}{r}\right)\,dy\,dx
\end{aligned}
$$

(where the first equality follows from the change of variables $u=x-\delta$), which is exactly ORS^2 applied to an infinitely long, thin "mesa" of constant height H. This in turn can be estimated as follows, using Lemma 8:

$$
\begin{aligned}
\int_{-\frac{\delta}{2}}^{\frac{\delta}{2}}\int_{-\infty}^{\infty} f^2\left(\frac{H}{r}\right)\,dy\,dx &= \int_{-\frac{\delta}{2}}^{\frac{\delta}{2}}\int_{-\frac{\delta}{2}}^{\frac{\delta}{2}} f^2\left(\frac{H}{r}\right)\,dy\,dx\\
&\quad +2\int_{-\frac{\delta}{2}}^{\frac{\delta}{2}}\int_{\frac{\delta}{2}}^{H} f^2\left(\frac{H}{r}\right)\,dy\,dx\\
&\quad +2\int_{-\frac{\delta}{2}}^{\frac{\delta}{2}}\int_{H}^{\infty} f^2\left(\frac{H}{r}\right)\,dy\,dx\\
&\le 2\pi\int_{0}^{\frac{\sqrt{2}}{2}\delta} f^2\left(\frac{H}{r}\right)\,r\,dr\\
&\quad +2\delta\int_{\frac{\delta}{2}}^{H} f^2\left(\frac{H}{y}\right)\,dy\\
&\quad +2\delta\int_{H}^{\infty} f^2\left(\frac{H}{y}\right)\,dy\\
&\le 2\pi\cdot\frac{4}{\pi^2}H\cdot\frac{\sqrt{2}}{2}\delta\\
&\quad +2\delta\cdot\frac{4}{\pi}\cdot H\cdot\ln\left(\frac{2H}{\delta}\right)\\
&\quad +2\delta\cdot\frac{2}{\pi^3}\cdot\frac{H}{3}
\end{aligned}
$$

Hence we have

$$
\mathrm{ORS}^2(\delta,0,0;h)-\mathrm{ORS}^2(0,0,0;h)\to 0 \quad \text{as} \quad \delta\to 0 \ \ (\text{with } H \text{ fixed})
$$

so ORS^2 and ORS are continuous in $\mathbf{p}$. Since the bound we derived only depends on H, and not on $\mathbf{p}$, h, or h_0, the continuity is uniform as desired. ■

(Note: if we put a bound on the slope of h near $\mathbf{p}$, this can be sharpened to yield Lipschitz continuity.)

We are usually interested in the case where $h_0=h(\mathbf{p})$, yielding the function (with h fixed and $\mathbf{p}$ variable) $\mathrm{ORS}(\mathbf{p},h(\mathbf{p});h)$. Note that in general (when h is not continuous) we do not expect this function of $\mathbf{p}$ to be continuous, since the reference height follows the discontinuous function h. However, wherever h is continuous, Theorem 17 and Corollary 13 together imply that $\mathrm{ORS}(\mathbf{p}, h(\mathbf{p}); h)$ will also be continuous.

3 Examples

To get a feel for the meaning of ORS, it is most instructive to look at explicit examples, preferably with pictures. Below we display a sample cross-section for a few representative peaks. In addition, the Peaklist website [5] and viewing packages such as Google Earth[9] are very useful. All of the ORS values for the examples were generated by computer, using gridded digital elevation models (DEMs).[10]

First let us dispatch our introductory contrasting examples, Mount Elbert and Devils Thumb. Mount Elbert has an ORS of 237 meters, while Devils Thumb's is 828 meters, corresponding to their dramatically different profiles as shown in Table 1. These values show that a comparison between these two peaks based on ORS gives the opposite result from the comparison suggested by their absolute elevations.

Another illustrative contrast is provided by Yosemite National Park. The highest point in the park is Mount Lyell, (Google Earth Tour) at 3999 meters. It has a respectable ORS value of 200 meters. See Table 2. However, far more famous is the huge granite cliff on the side of Yosemite Valley known as El Capitan (GE). It is hardly a mountain at all (there is higher terrain quite nearby), and its "summit" (a minor knoll some distance back from the brow of the cliff) has an elevation of only 2307 meters. El Capitan is a good example of a feature whose maximum ORS value is not obtained at the "summit" (local maximum of height). Rather, it is obtained by placing the reference point just atop the steepest portion of the cliff. The resulting ORS value is 575 meters. See Table 2. (The similarly famous and impressive Half Dome (GE) nearby gets an ORS of 580 meters; these are easily the two best ORS values in the park, and in the whole Sierra Nevada.) Here ORS clearly correlates much better with the notability of the features than does absolute elevation.

Table 3 lists the six U.S. states with the highest maximum ORS value. Not suprisingly, Alaska tops the list, although Mount McKinley (GE) (ORS = 1243 m, Elev = 6194 m) is not the best point in Alaska. The lower Mount Saint Elias (GE) is very close to tidewater (about 10 km away) , and is comparably steep, so it gets a higher ORS value. Most of the other peaks are well-known, except perhaps Mount Cleveland (GE), the high point of Glacier National Park. (The glaciers there are fast disappearing, but they have carved a number of

[9] However note that, as of 2013, in some regions (typically non-U.S. regions with high relief), the dataset that underlies Google Earth is still of varying, and sometimes strikingly low, quality.

[10] The typical accuracy of the ORS values presented in this section is a few percent. More details on the calculations can be found on the peaklist website.[5]

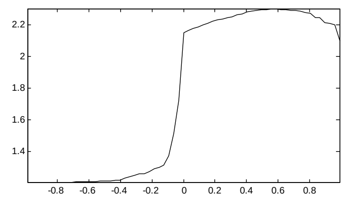

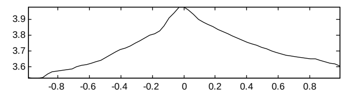

Table 2: El Capitan (left) and Mount Lyell (right) profiles

Peak	**ORS**	**Elev**	**State**
Mount Saint Elias (GE)	1334	5489	Alaska
Mount Rainier (GE)	827	4392	Washington
Grand Teton (GE)	683	4197	Wyoming
Mount Shasta (GE)	675	4317	California
Mount Cleveland (GE)	672	3190	Montana
Mount Hood (GE)	649	3452	Oregon

Table 3: State best points by ORS

exceptionally steep peaks.) It is interesting to also compare Mount Whitney (GE), the high point of the contiguous U.S. (ORS = 418 m, Elev = 4421 m); note that it is bested within California not only by the huge stratovolcano Mount Shasta (GE), but also by El Capitan and Half Dome (among others).

Worldwide, we have Table 4[11], which lists the top five independent[12] peaks in the world. Four are in the Himalaya, while Rakaposhi is in the nearby Karakoram range. While three of these peaks are in the famed group of fourteen "eight-thousanders" (with elevation over 8000 meters), two are not; in fact Machhapuchhare is not even in the top 300 peaks in the world by elevation. (It is a tremendously steep peak, near low terrain, in the Annapurna region of Nepal; it is highly sacred and is off-limits to climbing.) For comparison, Mount Everest, elevation 8848 m, gets a very respectable ORS value of 1302 m. Also note the dramatic difference in scale between these peaks and peaks in the contiguous U.S. (Mount Saint Elias does, however, come close to the top five, and actually beats Everest.)

[11] Since uniform topographic mapping is not available for these peaks, the links are to Google Earth tours. They give the general impression, but be aware that they are not always highly accurate.

[12] This list was actually generated by taking the five highest points as ranked by reduced ORS, as in Section 4, to ensure five truly independent peaks.

Peak	ORS	Elev	State
Nanga Parbat	1740	8125	Pakistan
Dhaulagiri	1680	8167	Nepal
Rakaposhi	1628	7788	Pakistan
Machhapuchhare	1596	6993	Nepal
Manaslu	1550	8163	Nepal

Table 4: World's top five independent peaks by ORS

4 Derived concepts

We have created two main concepts derived from ORS: *reduced ORS (RORS)* and *domain relief and steepness (DRS)*. We will discuss both briefly, without proofs.

RORS is used for building a list of the "best" peaks (as judged in terms of relief and steepness) in a region. Since, for a fixed, continuous landscape function h, $\mathrm{ORS}(\mathbf{p}, h(\mathbf{p}); h)$ is a continuous function of $\mathbf{p}$, it is nonsensical to compile a list of points with the highest possible ORS values in a given region. This is true of height, as well; lists of the "highest N peaks" in a given region usually use some cutoff criterion to eliminate trivial subpeaks. Instead of pursuing this strategy, we created RORS, which is a variant of ORS which takes into account the degree of independence of a given peak from nearby "better" peaks.[13] Hence it measures a combination of relief, steepness, and independence. For details, we refer the reader to [5], but we can briefly note the most important feature of RORS. It is *automatically discrete*: for any $\varepsilon > 0$, the set of points $\mathbf{p}$ with $\mathrm{RORS}(\mathbf{p}) > \varepsilon$ is discrete (and hence finite, in a bounded domain). This makes it a valid list-making criterion; the list of the top N points in a given region, as ranked by RORS, is meaningful. Various such lists are presented on the website [5].

The second concept derived from ORS is more straightforward to define. It is a measure of the ruggedness of a given domain, taking into account both relief and steepness. It is easy to create such a measure using ORS: roughly, we (RMS) average the ORS value for every point in the domain, yielding what we call *domain relief and steepness*, DRS. However there are two additional issues. First, given a bounded domain $K \subset \mathbb{R}^2$, and a landscape function h, we redefine ORS to use sample points only within the given domain. Second, instead of declaring our modified slope integrand f to have $f(u) = 0$ for $u < 0$, we extend it as an even function.[14]

With notation as in Section 2, we define the new version of ORS, appropriate

[13] Part of the inspiration for this strategy was *topographic prominence*, a popular alternate mountain measure. See for example [6].

[14] This change is not essential, but it does make the resulting formula more symmetric. It is easy to verify that using the original convention for f instead results in a definition of DRS that is $1/\sqrt{2}$ times that given here.

to this setting, as

$$\begin{aligned}\mathrm{ORS}(\mathbf{p}, h_0; h, K) &= \|f \circ u\|_{2,K} \\ &= \left[\iint\limits_K f^2\left(\frac{h_0 - h(\mathbf{x})}{\|\mathbf{p}-\mathbf{x}\|}\right) dA(\mathbf{x})\right]^{1/2}\end{aligned}$$

Then we define

$$\mathrm{DRS}(h, K) = \left[\frac{1}{A(K)}\iint\limits_K ORS^2(\mathbf{p}, h(\mathbf{p}); h, K)\ dA(\mathbf{p})\right]^{1/2}$$

where $A(K)$ is the area of K. This can be expressed directly in terms of the (new) modified slope integrand f as follows. Abusing notation slightly, let $u(\mathbf{p}, \mathbf{x}) = (h(\mathbf{p}) - h(\mathbf{x})) / \|\mathbf{p}-\mathbf{x}\|$. Then

$$\begin{aligned}\mathrm{DRS}(h, K) &= \frac{1}{\sqrt{A(K)}}\|f \circ u\|_2 \\ &= \left[\frac{1}{A(K)}\int\limits_{K\times K} f^2\left(\frac{h(\mathbf{p}) - h(\mathbf{x})}{\|\mathbf{p}-\mathbf{x}\|}\right) dA(\mathbf{p})\ dA(\mathbf{x})\right]^{1/2}\end{aligned}$$

Note that this (quadruple) integral is symmetric in the variables $\mathbf{p}$ and $\mathbf{x}$, and that it has units of length, just as ORS does (recall that f is dimensionless).

We will not go into detail regarding DRS here; see [5] for more. However we will make two notes about it.

First, DRS is sensitive to the overall slope of the terrain, but it is continuous in the L^∞ norm, unlike a functional based on derivatives. Hence it will not give an unreasonably high value to a landscape with low relief, no matter how rugged, nor will its value depend (absurdly) on a particular microscale model of matter. (Think of applying the derivative to the surface of a “flat”, “level” table, but taking into account the atomic-scale bumpiness of the surface—one will not obtain the expected value of zero.)

Second, empirical investigations indicate that the following problem is well-defined (with perhaps some mild regularity assumptions): within a given domain K_0, what is the domain $K \subset K_0$ with maximal ruggedness? Doing this is a tricky problem in calculus of variations, one which we have not investigated completely. However a coarse-gridded numerical approximation to this problem yields stable results. For example, our calculations indicate that the most rugged region in the contiguous 48 states is the Picket Range (GE) of the North Cascades, in Washington State.[5]

5 Future work

There are several directions which we expect to pursue to extend this work. First is the continued measurement and tabulation of the world's mountain topography, aided by the progressive improvement in availability of digital data for regions outside the United States. Second are theoretical issues such as dealing with overhanging terrain for ORS and the problem of finding optimally rugged regions for DRS. Third is the possible application of these ideas to image analysis. A grayscale image, for example, is usually modeled as a real-valued function of two variables, to which our functionals could apply. It would be interesting to see if ORS, RORS, and DRS could be used to accomplish some of the standard tasks (or novel ones) in image analysis.

6 Acknowledgements

The seed of the idea of ORS came from Bob Bolton. He and other members of the Prominence electronic discussion group contributed a great deal of feedback to the early work on ORS (then known as "spire measure"). Data sets for the computer calculations of spire measure (done in MATLAB) primarily came from the National Elevation Dataset (U.S.), Canadian Digital Elevation Data (Canada), and the Shuttle Radar Topography Mission (worldwide)—the last with major, invaluable improvements due to Jonathan de Ferranti.

References

[1] National Geodetic Survey Datasheets, http://www.ngs.noaa.gov/cgi-bin/datasheet.prl

[2] British Columbia GNIS Query Page, http://www.ilmb.gov.bc.ca/bcgn-bin/bcg10?name=25218

[3] V. M. Tikhomirov, Gâteaux variation, in Hazewinkel, Michiel, *Encyclopedia of Mathematics*, Springer-Verlag, New York, 2001, available at http://eom.springer.de/G/g043390.htm

[4] J. Dieudonné, *Treatise on Analysis, Volume II* (translated from the French by I. G. MacDonald), Academic Press, New York, 1970, p. 124.

[5] Peaklist website, ORS section: http://peaklist.org/spire/

[6] "Topographic Prominence", http://en.wikipedia.org/wiki/Topographic_prominence

SOLSTICE:
An Electronic Journal of Geography and Mathematics

Persistent URL:
http://deepblue.lib.umich.edu/handle/2027.42/58219

Cite articles as:
Author names(s), Year. Title of article, *Solstice: An Electronic Journal of Geography and Mathematics*, Vol. XX, No. YY. Ann Arbor: Institute of Mathematical Geography.

VOLUME XXIV, NUMBER 2;
December, 2013

Klein 4 Group: Beth Olem Cemetery Application

Sandra Lach Arlinghaus

Introduction: A Cemetery Inside the Grounds of an Auto Plant

A number of years ago, in the mid-1980s, General Motors Corporation built the Detroit/Hamtramck Assembly plant near the intersections of major Detroit freeways and major rail lines. Proximity to transportation links made sense from a variety of viewpoints. To acquire the land for the large new plant (eventually to cover 362 acres), a combination of deals were employed (eminent domain, purchase, and so forth); some met with more favor than did others (Wikipedia).

The Detroit/Hamtramck Assembly Plant, has extensive security surrounding it. Figure 1 shows a secured entrance gate. Figure 2 shows the general location of the plant, at the north end of Chene Street, in the contemporary context of Google Earth.

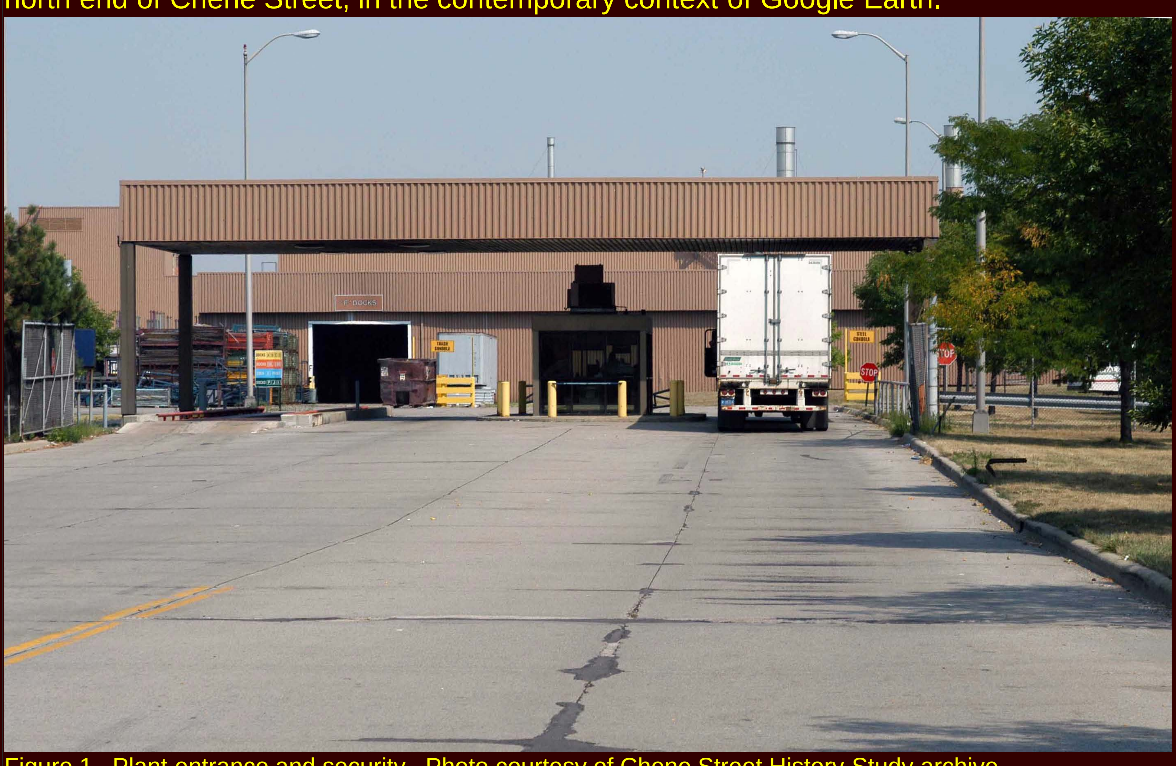

Figure 1. Plant entrance and security. Photo courtesy of Chene Street History Study archive.

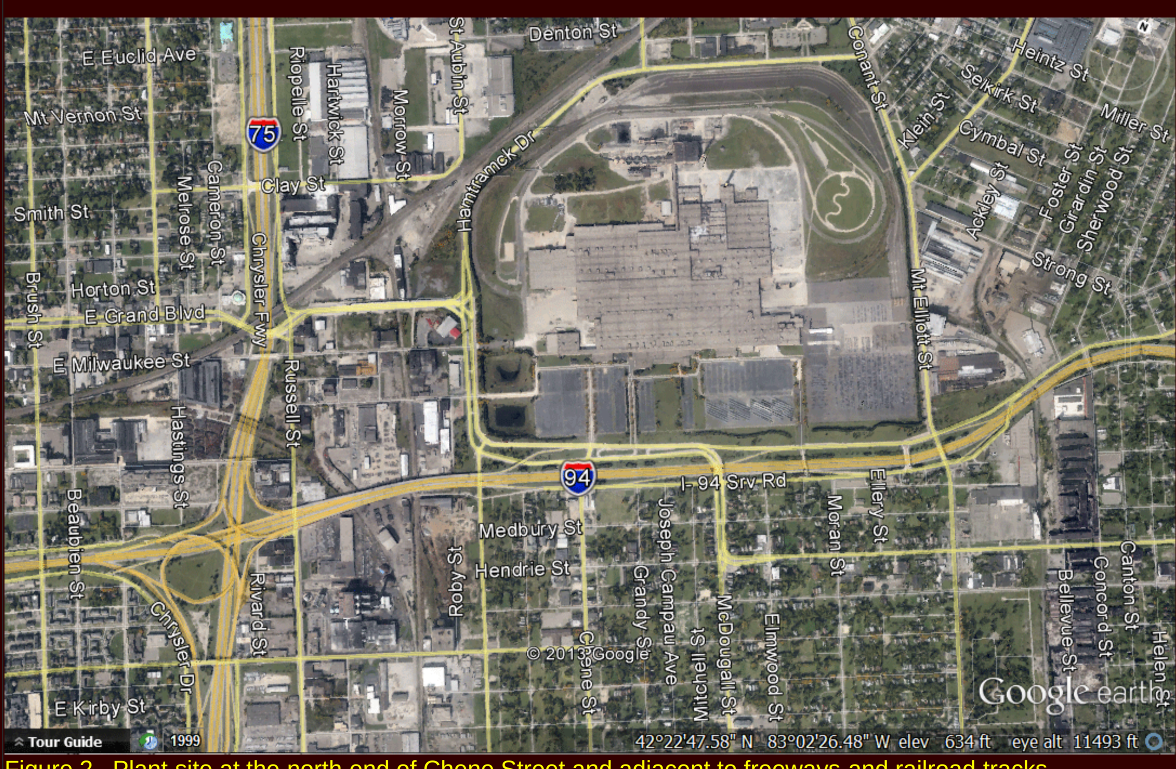

Figure 2. Plant site at the north end of Chene Street and adjacent to freeways and railroad tracks.

Take a closer look; the area to the north end of the plant contains quite a bit of grass adjacent to the giant parking lot. Figure 3 shows a small patch of trees that appear more mature than the others on the plant site. The trees appear walled into a rectangular area.

Figure 3. Rectangular patch of mature trees behind a wall.

The patch of trees is, in fact, part of a cemetery that predated, by almost a century, the Detroit/Hamtramck Assembly Plant. General Motors was not able to acquire that small patch of land because of zoning and easement restrictions already in place in association with the cemetery. Figure 4 shows a closer look at the cemetery.

Figure 4. Cemetery on the grounds of the Detroit/Hamtramck Assembly Plant. Note tombstones. Entrance gate is to the left of the white car.

Records in the Chene Street History Study (CSHS) and elsewhere show that this cemetery is named Beth Olem and that it is a Jewish cemetery that is one of the oldest in Michigan. It is open for only a few hours a year, in association with selected Jewish holidays. To visit the grave of a loved one, it is required to enter through GM security first (Figure 1) and then through cemetery security which requires the gates of the walled cemetery to be open. The walls are 8 feet tall. Naturally, this high level of security makes it difficult for visitors to gain access.

Comtemporary Visualization: Virtual Beth Olem Cemetery

Google Earth or other contemporary visualization technology could make it possible, however, to overcome the frustrating security situation. Imagine a 3D model of the cemetery, complete with geo-referenced images/models of tombstones. Click on a grave marker and get taken to materials from the archive (insofar as privacy concerns permit). Link from the tombstone to a blog of associated materials. The process of building a virtual Beth Olem is underway. When complete, it will serve not only to overcome access and distance issues for loved ones to visit 24/7, but it will also serve as a basic study in the systematic use (by blog associations) of the CSHS archive, added to the present 'GEOMAT' (Geographic Events Ordering: Maps, Archives, Timelines; Arlinghaus, Haug, and Larimore) methodology.

The archives of the Chene Street History Study have many photos taken from inside Beth Olem. The image in Figure 5 is one example that shows clearly the proximity of the industrial complex to the otherwise peaceful resting ground; the juxtaposition of the different worlds is really quite startling.

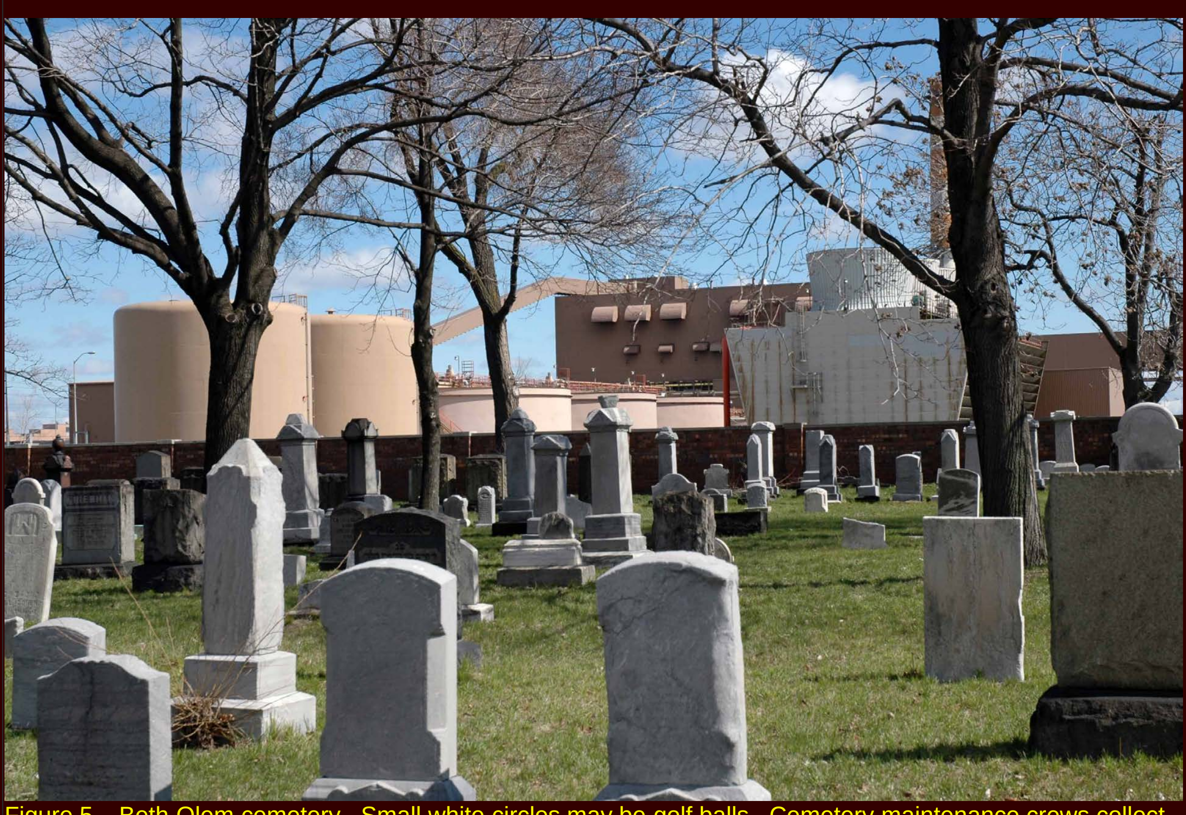

Figure 5. Beth Olem cemetery. Small white circles may be golf balls. Cemetery maintenance crews collect golf balls from the grounds that executives apparently hit at lunchtime into the cemetery from nearby parking lots. Photo courtesy of Chene Street History Study archives.

The cemetery is no longer taking new 'residents.' In that regard, it offers to researchers an advantage similar to the opportunity offered to foreign language students who begin by studying Latin (or another 'dead' language). There is no (or little) change--the 'syntax' and 'grammar' of the situation are frozen. These are true anchors for process and a fine place to begin study, prior to moving out, in this case to the more dynamic setting of the changing urban Chene Street scene.

A First Step in Creating the Virtual Beth Olem: The Walls

The cemetery is a compact entity that is easy to deal with geometrically: it is a rectangle. The walls around it delineate it clearly and make it quickly recognizable. In terms of creating a virtual cemetery, the walls serve as a good starting point. Once the walled boundary is created, then infill can proceed with the walls as guides to reduce placement error. Accuracy in placement of the walls is straightforward: it is easy to read off the latitude and longitude from a smartphone camera used to take a photo next to the wall. General placement is straightforward from tracing the footprint in Google Earth. What is a challenge with modeling the walls is getting the surface to look correct so that the created visualization is realistic.

Surface Pattern

It is a simple matter to capture a swatch of the pattern on the walls from a photograph. However, it is not possible to use that swatch, only, to create the full wall--at least not in a realistic manner. In Figure 6a, a single swatch of an arbitrary pattern is used to tile a broad area; the visual effect is not satisfactory. One has a sense that the single tile might be employed to greater advantage; blue and orange pattern do not align as the walls are tiled (Figure 6b). The tiling of a plane using geometric shapes is called a tessellation (see Wikipedia reference).

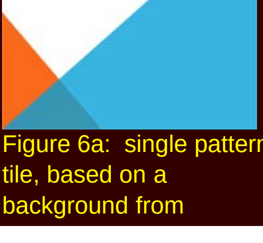

Figure 6a: single pattern tile, based on a background from

MicroSoft PowerPoint.

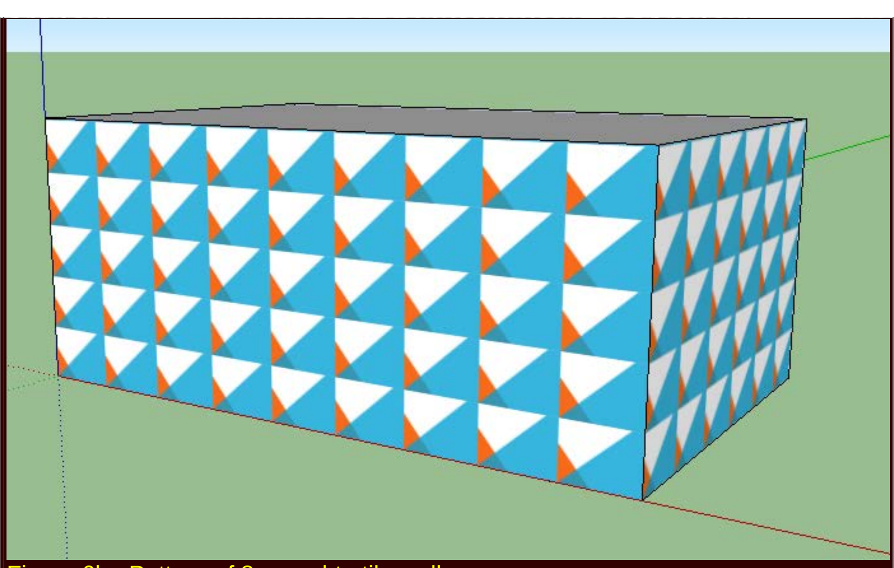

Figure 6b. Pattern of 8a used to tile walls.

To improve alignment and consequent appearance and visual impression, one might flip the single tile or rotate it to create different patterns and then align it with the base tile of Figure 6a to create a larger single tile to tile the walls with. Figure 7 shows a flip about a vertical axis in animated fashion. Figure 8a shows the flipped tile appended to the base tile; Figures 8b, and 8c illustrate the resulting pattern when 8a is applied to the walls of a box.

Figure 7. Flip of tile about a vertical axis.

In Figure 8b, the applied pattern has alignment issues resolved in horizontal strips but not from top to bottom. Figure 8c suggests that this single flip is sufficient to optimize visual alignment if the tile covers the wall from top to bottom.

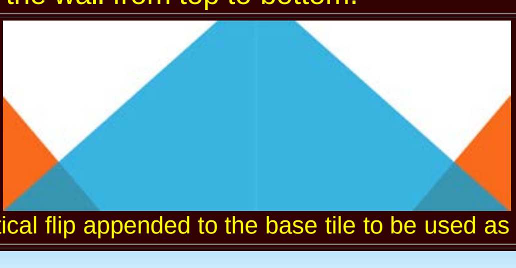

Figure 8a. Tile with a vertical flip appended to the base tile to be used as a new tile for tiling a wall.

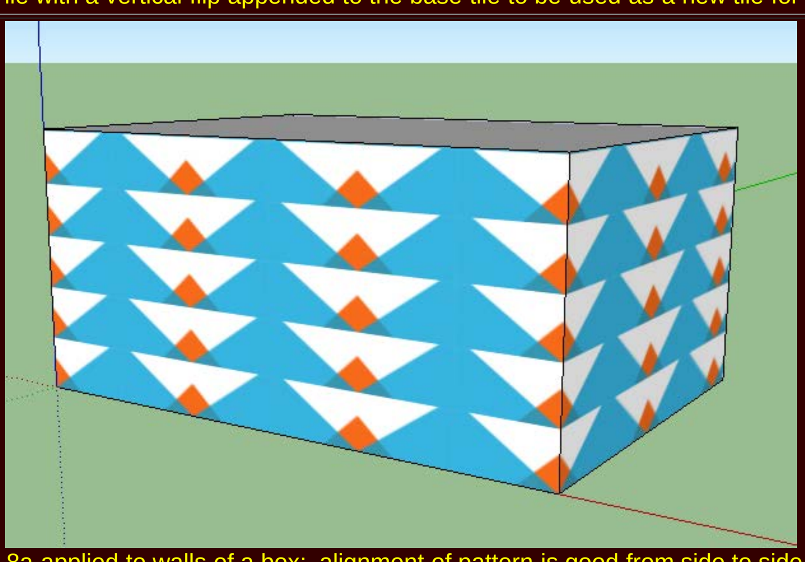

Figure 8b. Tile of 8a applied to walls of a box: alignment of pattern is good from side to side but not from top to bottom.

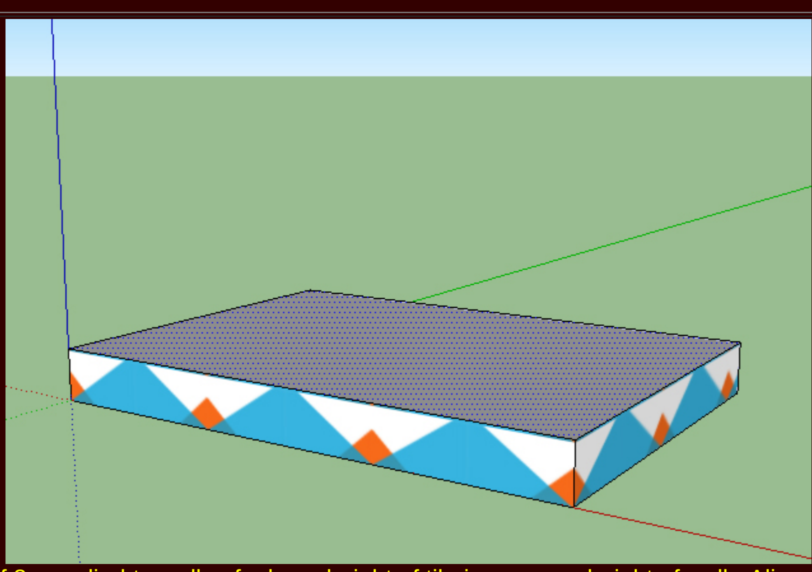

Figure 8c. Tile of 8a applied to walls of a box: height of tile is same as height of wall. Alignment is good both from side to side and from top to bottom.

In the case of the walls at Beth Olem, the situation of Figure 8c prevails; it is possible to find a swatch from top to bottom. Figure 9 shows the results of a model created in Trimble SketchUp. The edges along the tops of the walls, as well as the dots in the walls, align across the entire wall. Look at the grass stains on the bottom to see where the vertical flip was made. Figure 10 confronts the model with the reality of a photograph. There are no grass stains on the outsides of the walls. The reason there are grass stains on the modeled walls is that images from the interior side of the walls were used as textures on the outsides; use of actual images of the exterior required excessive removal of tree limbs not present when the interior images were used. Evidently, there are varying degrees of wetness at different times of the year. A similar strategy of using a view from the inside, and then flipping it, was employed with the sign for the cemetery, again so that it too might be disentangled from the tree limbs. One might further refine the detail of images; that action, however, has nothing to do with establishing process.

Figure 9. Beth Olem walls, model.

Figure 10. Beth Olem Cemetery entrance. Photo courtesy of Chene Street History Study archives.

In the situation above, a flipped tile was appended to one side of a base tile. Naturally, the flipped tile might also be applied to each of the other three sides to create other tiling patterns. The one selected to be exhibited is one that works well for modeling the Beth Olem walls. Thus, the first step in wall completion is solved. But, to learn more from this 'anchor' case, consider other possibilities.

The Klein 4 Group: Pattern Alignment Issues

The case above employed a vertical flip of a rectangular (non-square) base tile to create a new larger tile by appending the flipped tile to one side of the base tile; it was an exercise in 'spatial mathematics' (Arlinghaus and Kerski). What other transformations of the base tile might be employed to create other larger tiles that improve tiling alignment issues on a wall? Clearly, one might flip the base tile about a horizontal axis. Further, one might rotate the base tile through 180 degrees and still maintain tile orientation. Figure 11a-d illustrates these possibilities.

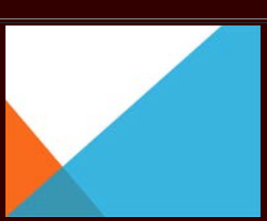

Figure 11a. Base tile

Figure 11b. Vertical flip

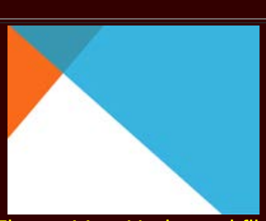

Figure 11c. Horizontal flip

Figure 11d. 180 degree flip

Because the base tile is non-square, rotation through 90 degrees will not maintain tile orientation; the 'landscape' tile will rotate to a 'portrait' tile under such a transformation. Are there, however, other rigid motions (see Wikipedia reference) of a non-square rectangle that will yield new pattern? Intuitively, the answer appears to be 'no'. It is possible to prove that answer using a structure from a branch of mathematics called group theory.

To introduce appropriate notation, replace the visual pattern in the non-square rectangles with numerical pattern, labelling the vertices of the rectangles as 1, 2, 3, 4. Thus the sequence in Figure 13a-d is replaced by the sequence in Figure 12a-d.

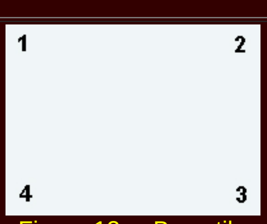

Figure 12a. Base tile

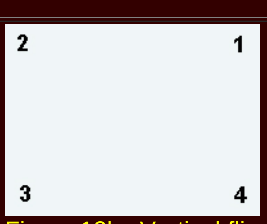

Figure 12b. Vertical flip

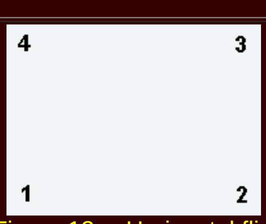

Figure 12c. Horizontal flip

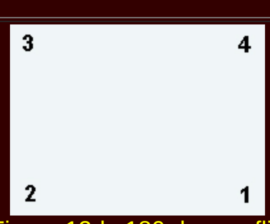

Figure 12d. 180 degree flip

To illustrate how to use the numbers, represent the base tile as the identity permutation on these four numbers: (1)(2)(3)(4). Represent the vertical flip as: (12)(34), read perhaps as '1 goes to 2' then once the end of a parenthetical notational phrase is reached, the last element 'goes' to the first one, so here '2 goes to 1'. Similarly, represent the horizontal flip as: (14)(23). Finally, represent the 180 rotational flip as (13)(24). Does this set of permutations form a closed system? If so, then there are no other possible rigid motions to use to generate larger tiles from the base tile.

A 'group' is a mathematical structure that may exist on a set of elements with one operation. When elements are combined using that operation, the system is said to be a group if it is closed (no new elements are generated), if it is associative (grouping using parentheses is clear: a(bc)=(ab)c), if there is an identity property: a*I = a, and if there is a unique inverse for each element: $a*a^{(-1)}$ = I. In the case of the permutations representing rigid motions of a non-square rectangle I = (1)(2)(3)(4). The operation, *, involves combining permutations as below.

> (12)(34)*(13)(24) is executed as starting on the left (for example) with 1--in the first permutation, 1 goes to 2; in the second permutation, 2 goes to 4. Thus, in the resulting product, 1 goes to 4 or (14. Now, where does 4 go? Start in the first permutation--4 goes to 3 and in the second permutation, 3 goes to 1. Thus, in the resulting product, 4 goes to 1 so it is now correct to close the parentheses (14). Now go back to the first permutation to see where 2 goes. In the first permutation, 2 goes to 1; in the second permutation, 1 goes to 3. So, in the result, 2 goes to 3: (23 . Then go back to the first permutation where 3 goes to 4 and then in the second permutation 4 goes to 2. Thus, 3 goes to 2 and it is correct to close the parentheses: (23).

Thus, (12)(34)*(13)(24) = (14)(23). With a bit of practice, one can perform this operation quickly. Look at a table composed of all possible permutation 'multiplications' (Figure 13). The column on the left is the set of 'first' permutations; the row across the top is the set of 'second' permutations

*	(1)(2)(3)(4)	(12)(34)	(14)(23)	(13)(24)
(1)(2)(3)(4)	(1)(2)(3)(4)	(12)(34)	(14)(23)	(13)(24)
(12)(34)	(12)(34)	(1)(2)(3)(4)	(13)(24)	(14)(23)
(14)(23)	(14)(23)	(13)(24)	(1)(2)(3)(4)	(12)(34)
(13)(24)	(13)(24)	(14)(23)	(12)(34)	(1)(2)(3)(4)

Figure 13. Group table, Klein 4 Group.

Verify that no new elements were created: all are displayed in the table. Verify that the associative law holds: for example, (12)(34)*[(13)(24)*(14)(23)] is the same as [(12)(34)*(13)(24)]*(14)(23). Show for each grouping; begin by working from within sets of parenthetically enclosed permutations. It is straightforward from the table that (1)(2)(3)(4) is an identity element; it is also straightforward from the table that there is no other identity element. Finally, read the table to see that each element is its own inverse: (12)(34)*(12)(34) = (1)(2)(3)(4), for example. Thus, this set of four permutations, representing rigid motions of a non-square rectangle, forms a group. It was discovered by Felix Klein and is referred to as the Klein 4-Group (Vierergruppe) and is often denoted V.

Thus, because the group structure is verified, there are no other patterns of the sort above, based on a non-square rectangle, that can be used to generate wall tiling. Of course, one can improve pattern alignment by using a larger tile, such as the one in Figure 8a, and flipping that to create an even larger base tile. Figures 14a-c suggest one such strategy: apply a vertical flip to the base tile, append that to the base tile (Figure 14a) then apply a horizontal flip to the tile in 14a to create a larger tile in Figure 14b. This new tile, as shown in Figure 14c, will combine both the good side-to-side alignment and top-to-bottom alignment of the vertical and horizontal flips. The tile is new, and the alignment pattern of wall tiling is new and improved; however, there is no new motion involved, as the Klein 4 Group shows.

Figure 14a. Vertical flip of base tile appended to base tile

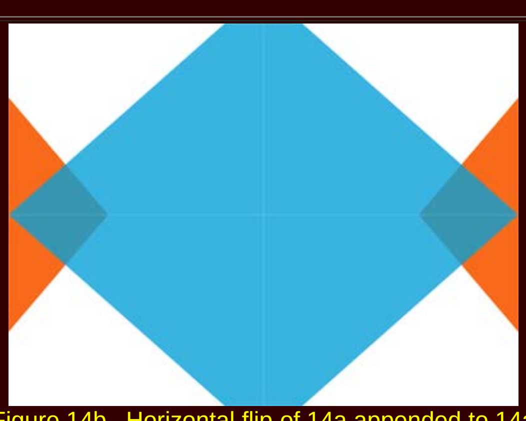

Figure 14b. Horizontal flip of 14a appended to 14a

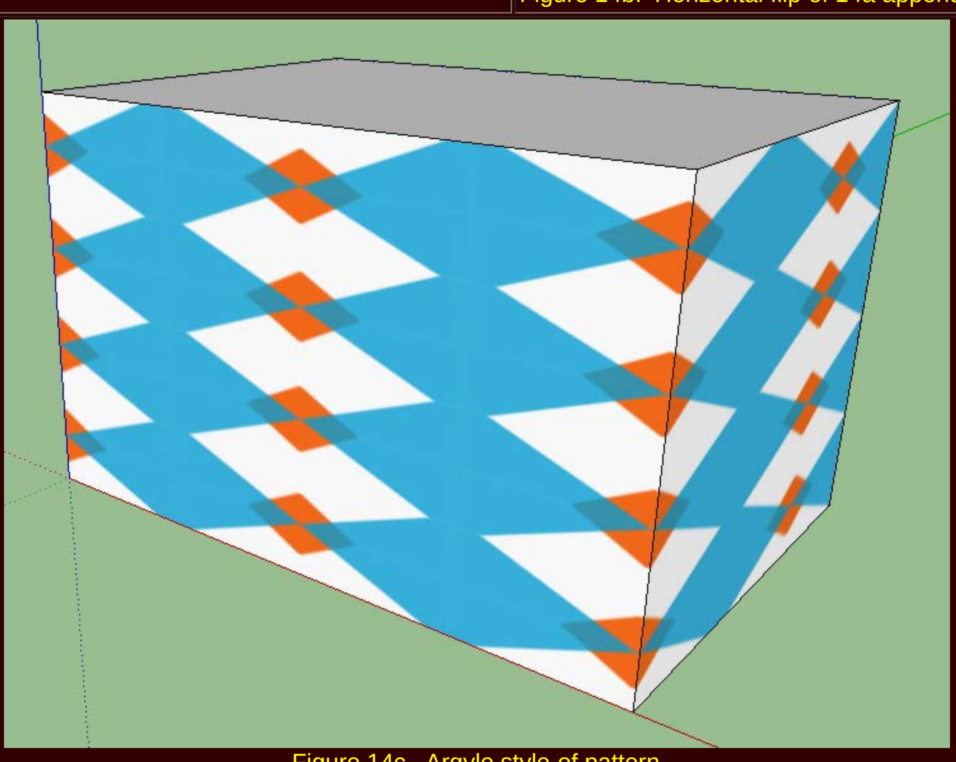

Figure 14c. Argyle style of pattern

Here, only a simple non-square rectangular tile was considered. One might carve out pieces of a rectangular tile and glue them on top or bottom or sides and create oddly-shaped Escher-like fish that fit together perfectly in two different directions and at different scales. The process is similar and employs the same general style of reasoning. One may use the chain of reasoning for non-Euclidean as well as Euclidean objects (see comments in the Escher Wikipedia reference involving the Escher 'Circle Limit series). The subjects of group theory and of tiling are deep ones--group theory lies at the theoretical root not only of simple tiling such as that shown here but also at that root of any tiling (see for example, Wikipedia, 'Wallpaper group'). References for further reading are suggested at the end of this document.

References Cited

Archive, Chene Street History Study, The University of Michigan, Ann Arbor.

Arlinghaus, Sandra L. and Kerski, Joseph. 2013. *Spatial Mathematics: Theory and Practice through Mapping*. Boca Raton: CRC Press.

Arlinghaus, S., Haug, R., and Larimore, A. Nov. 2011. *GEOMAT Guide: Directions for Building a GEOMAT Web Architecture for any Investigation or Case Study*. http//:www.geomats.org/

Krzyzowski, Marian. Director, Chene Street History Study; Director, Institute for Research on Labor, Employment, and the Economy, The University of Michigan, Ann Arbor.

Team (2013), Chene Street History Study. Marian Krzyzowski (Director), Karen Majewska (Ph.D. History and current Mayor, Hamtramck Michigan), Sandra Arlinghaus, Ann Larimore, Hannah Litow, Shera Avi-Yonah.

Wikipedia.
Detroit/Hamtramck Assembly:
http://en.wikipedia.org/wiki/Detroit/Hamtramck_Assembly
Tesselation: http://en.wikipedia.org/wiki/Tessellation

M. C. Escher: http://en.wikipedia.org/wiki/M._C._Escher
Rigid Motions, Euclidean Group: http://en.wikipedia.org/wiki/Euclidean_group

Software Used

Adobe PhotoShop
Google Earth
MicroSoft Office, PowerPoint, Word.
Trimble SketchUp

References for further reading

Birkhoff, G. and Mac Lane, S. 1961. *A Survey of Modern Algebra*. New York: MacMillan.

Coxeter, H. S. M., 1961, *Introduction to Geometry*. New York: MacMillan.

Coxeter, H. S. M., Emmer, M., Penrose, R., and Teuber, M. L. eds. 1986. *M. C. Escher: Art and Science*. Amsterdam: North-Holland.

Grünbaum, Branko and Shephard, G. C. 1987. *Tilings and Patterns*. New York: Freeman.

Herstein, I. N. 1975. *Topics in Algebra*, New York: Wiley.

Loeb, Arthur. 1976. *Space Structures: Their Harmony and Counterpoint*. Reading, MA: Addison-Wesley.

Schattschneider, Doris (June/July 2010). "The Mathematical Side of M. C. Escher" (PDF). *Notices of the American Mathematical Society* (USA) 57 (6): 706–18.

Weyl, Hermann. 1952. *Symmetry*. Princeton: Princeton University Press.

Wikipedia:
Group: http://en.wikipedia.org/wiki/Group_%28mathematics%29
Group Theory, http://en.wikipedia.org/wiki/Group_theory
Klein Four-group, http://en.wikipedia.org/wiki/Klein_four-group

Remembering those who are gone now but who contributed in various ways to *Solstice* or to IMaGe projects, directly or indirectly, during the first 28 years of IMaGe:

Allen K. Philbrick Alma S. Lach Donald F. Lach | Frank Harary | William D. Drake | H. S. M. Coxeter | Saunders Mac Lane | Chauncy D. Harris | Norton S. Ginsburg | Sylvia L. Thrupp | Arthur L. Loeb | George Kish |

1964 Boulder Drive,
Ann Arbor, MI 48104
734.975.0246
http://deepblue.lib.umich.edu/handle/2027.42/58219
sarhaus@umich.edu

SOLSTICE:
An Electronic Journal of Geography and Mathematics

Persistent URL:
http://deepblue.lib.umich.edu/handle/2027.42/58219

Cite articles as:
Author names(s), Year. Title of article, *Solstice: An Electronic Journal of Geography and Mathematics*, Vol. XX, No. YY. Ann Arbor: Institute of Mathematical Geography.

Deep Blue IMaGe Home Solstice Home

VOLUME XXIV, NUMBER 2;
December, 2013

GEO-MUSIC: LINKED SELECTIONS

Sandra Lach Arlinghaus

The Earth inspires us in different ways; some respond to the beauty of the sun setting beyond the spherical horizon with quiet admiration while others respond in their own special ways to the boldness and grandeur of a mighty river. Our responses are of course conditioned by what we know and practice in our daily lives. Consider the response of music composers not only to nationalistic pride and place names, but also awe-inspiring rock formations, environmental issues, political situations, cultural backdrop, and so forth. Please add to this list by sending me, via email (sarhaus@umich.edu), your own favorites and we'll accumulate them in a later issue of *Solstice* as a sort of geo-musical atlas. An earlier Solstice article suggested a different context for this sort of idea (Arlinghaus, S. and Blake, B., "Two Rivers Ridge: Capturing Art, *Solstice*, Volume XV, No. 2., 2004).

Is music inspired by the Earth somehow more moving to you than other pieces, independent of genre? Others have noted similar ideas; but, as geography is more than place names--so too is a musical response to patterns on, or seen from, the Earth's surface. Here are links to a few sites listing place name music, elsewhere on the Internet. An additional list follows reflecting the abundance of geo-music beyond place name music, supplemented when it seemed natural, with related poetic quotations.

Added inspiration is often fostered in museums. Consider, for example, the Musical Instrument Museum in Phoenix, AZ (http://mim.org/). Visit instruments, played in the field, from around the world and organized by continent and region within the walls of the museum, often with associated fabrics, costumes, You Tubes of indigenous population playing the displayed instruments in natural settings, and more. Visit the Experience Room and try your hand, along with others, on a variety of instruments. The author is shown below trying her hand with portions of the Indonesian Gamelan interactive display!

Photo by Barbara Grantham, November, 2013.

LINKS ELSEWHERE

- Magle International Music Forums
- Songs with Names of Cities in the Title
- Songs with Place Name in Title

COUNTRIES

- Felix Mendelsohn, Italian Symphony
- Jean Sibelius, Finlandia
- Johann Strauss II, Spanischer Marsch
- ________________________________
- Joan Baez, Don't Cry for Me Argentina
- Vic Damone, April in Portugal
- Paul Simon and Art Garfunkel, America

REGIONS

Jean Sibelius, Karelia Suite--Intermezzo
Felix Mendelsohn, Hebrides Overture
____
Don McLean, American Pie

CITIES

- Felix Mendelssohn, Venetianisches Gondellied
- Wolfgang Amadeus Mozart, Symphone No. 31 K. 297, D major, Paris
- Wolfgang Amadeus Mozart, Symphony No. 36 in C, K. 435, Linz Symphony
- Ottorino Respighi, Fountains of Rome
- Ottorino Respighi, Pini di Roma
- Johann Strauss II, Vienna Blood Waltz
- Richard Wagner, Die Meistersinger von Nürnberg, Overture
- ________________________________
- Joan Baez, House of the Rising Sun
- Tony Bennett, I Left my Heart in San Francisco
- Glen Campbell, By the Time I Get to Phoenix
- Glen Campbell, Galveston
- Nat King Cole, On the Sidewalks of New York
- George Gershwin, An American in Paris, Gene Kelly, I Got Rhythm
- Jerome Kern and Oscar Hammerstein III, Last Time I Saw Paris
- Guy Mitchell, There's a Pawn Shop on the Corner
- Frank Sinatra, Chicago, Chicago
- Meredith Willson, The Music Man, Gary, Indiana

WATER

- Ferde Grofé, Mississippi Suite
- Bedrich Smetana, Die Moldau
- Russian Song, The Song of the Volga Boatman
- Franz Schubert, Die Forelle, Dietrich Fischer-Dieskau, Moore.
- Johann Strauss II, The Blue Danube Waltz
- ________________________________
- Paul Dresser, On the Banks of the Wabash Far Away, Shannon Quartet
- Jerome Kern and Oscar Hammerstein III. Ol' Man River, Paul Robeson
- Marty Robbins, Red River Valley
- Pete Seeger, Michael Row the Boat Ashore
- Paul Simon and Art Garfunkel, Bridge over Troubled Water
  - *"I never saw a moor, I never saw the sea, Yet know I how the heather looks, And what a wave must be."* Emily Dickinson.
- Arthur Sullivan and W. S. Gilbert, Pirates of Penzance

WOODS AND FLOWERS

- Edvard Grieg, Peace of the Woods
- Franz Schubert / Johann Wolfgang von Goethe, Heidenröslein
  - *"I wandered lonely as a cloud, That floats on high o'er vales and hills, When all at once I saw a crowd, A host of golden daffodils. Beside the lake, beneath the trees; Fluttering and dancing in the breeze. ... Ten thousand saw I at a glance, Tossing their heads in sprightly dance."* William Wordsworth
- Johann Strauss II, Tales from the Vienna Woods

LANDFORMS

- Ferde Grofé, Grand Canyon Suite, Sunset
- ________________________________
- Bing Crosby and the Andrews Sisters, Don't Fence Me In
- John Denver, Rocky Mountain HIgh

TRANSPORTATION

- Roy Acuff, The Wabash Cannonball
- Rosemary Clooney, On the Atchison, Topeka, and the Santa Fe
- John Denver, Leaving on a Jet Plane
- Steve Goodman, City of New Orleans, sung by Willie Nelson
- Kingston Trio, M.T.A.
- Gordon Lightfoot, The Wreck of the Edmund Fitzgerald
  - " *'God save thee, ancient Mariner! From the fiends, that plague thee thus!—Why look'st thou so?'—With my cross-bow I shot the ALBATROSS.*" Samuel Taylor Coleridge
- Pete Seeger, The Erie Canal

CULTURAL BACKDROP AND POLITICAL

- Johannes Brahms, Hungarian Dance No. 5
- Antonin Dvorak, Symphony No. 9 in E Minor, from the New World
  - Adaptation, Going Home
- Giuseppe Verdi, Triumphal March, Aida
- ________________________________
- Joan Baez, The Night they Drove Ol' Dixie Down
- Joan Baez, We Shall Overcome
- Richard Rodgers and Oscar Hammerstein II, The King and I, March of the Siamese Children
- Buffy Sainte-Marie, Universal Soldier
  Paul Simon and Art Garfunkel, Scarborough Fair
- Andy Williams, Battle Hymn of the Republic

UTOPIAN

- Judy Garland, Over the Rainbow
- Burl Ives, Big Rock Candy Mountain

SEASONS, EARTH-SUN RELATIONS, DIRECTIONS

- Wolfgang Amadeus Mozart, Die Zauberflöte, The Magic Flute (Die Strahlen der Sonne Vertreiben die Nacht)
- Franz Schubert, Winterreise, Fischer-Dieskau, Brendel
- Johann Strauss II, Morgenblätter
- Johann Strauss II, Rosen aus dem Sũden
- Johann Strauss II, Voices of Spring Waltz
- Antonio Vivaldi, Four Seasons
- ________________________________
- Peter, Paul, and Mary. Blowing in the Wind
- Edith Piaf, Milord
  - *"The North wind doth blow, And we shall have snow, And what will the robin do then, Poor thing?"* Mother Goose
- Dinah Shore, Buttons and Bows
  - *"Oh, East is East and West is West, And never the 'twain shall meet."* Rudyard Kipling

EARTH IN SPACE

- Ludwig van Beethoven, Moonlight Sonata, Vladimir Horowitz
- Antonin Dvorak, Song to the Moon
- Gustav Holst, The Planets
- Wolfgang Amadeus Mozart, Symphony 41 (Jupiter) in C Major
- Wolfgang Amadeus Mozart: Ah, vous dirai-je Maman?
  - "Twinkle, twinkle little star, How I wonder what you are! Up above the world so high, Like a diamond in the sky." Jane Taylor

http://www.imagenet.org
http://deepblue.lib.umich.edu/handle/2027.42/58219

Solstice was a Pirelli INTERNETional Award Semi-Finalist, 2001 (top 80 out of over 1000 entries worldwide)

One article in Solstice was a Pirelli INTERNETional Award Semi-Finalist, 2003 (Spatial Synthesis Sampler).

Solstice is listed in the Directory of Open Access Journals maintained by the University of Lund where it is maintained as a "searchable" journal.

Solstice is listed on the journals section of the website of the American Mathematical Society, http://www.ams.org/

Solstice is listed in *Geoscience e-Journals*

IMaGe is listed on the website of the Numerical Cartography Lab of The Ohio State University: http://ncl.sbs.ohio-state.edu/4_homes.html

---

Congratulations to all *Solstice* contributors.

Remembering those who are gone now but who contributed in various ways to *Solstice* or to IMaGe projects, directly or indirectly, during the first 28 years of IMaGe:

Allen K. Philbrick Alma S. Lach Donald F. Lach | Frank Harary | William D. Drake | H. S. M. Coxeter | Saunders Mac Lane | Chauncy D. Harris | Norton S. Ginsburg | Sylvia L. Thrupp | Arthur L. Loeb | George Kish |

1964 Boulder Drive,
Ann Arbor, MI 48104
734.975.0246
http://deepblue.lib.umich.edu/handle/2027.42/58219
sarhaus@umich.edu